The Earth's Ionosphere

A. Zaslavsky

15 janvier 2026

Table des matières

1 Formation and structure of the ionosphere **2**
1.1 Photoionisation of the atmosphere 2
1.1.1 Zenith angle 2
1.1.2 Optical thickness of the atmosphere 5
1.1.3 Photoelectron production rate 6
1.1.4 Case of an isothermal atmosphere 6
1.2 Recombination processes 7
1.2.1 Radiative recombination 7
1.2.2 Dissociative recombination 8
1.2.3 Evaluation of electron density 8
1.3 Illustrations of the ionospheric structure 9
1.3.1 Isothermal model 9
1.3.2 The layers of the Earth's ionosphere 10

2 Transport phenomena **11**
2.1 Mobility and diffusion in a magnetised plasma 11
2.1.1 Expression of the conductivity 15
2.1.2 Order of magnitude of mobilities and conductivities in an isothermal atmosphere 16
2.2 Some effects of ionospheric transport 18
2.2.1 Ambipolar diffusion and plasma height scale 18
2.2.2 Electrodynamics of low latitudes : dynamo effect, Sq current system and equatorial electrojet 20
2.2.3 Electrodynamics of high latitudes : couplings to the solar wind and the magnetosphere 22

3 Bibliography **25**

1 Formation and structure of the ionosphere

In this section, we are interested in how the absorption of solar UV radiation leads to the formation of an ionised layer in the upper atmosphere. Let us begin by writing the equation of conservation of the number of electrons,

$$\frac{\partial n_e}{\partial t} + \mathrm{div}(n_e \mathbf{u}_e) = q_e - l_e. \tag{1}$$

On the right-hand side, it shows a source term q_e and a loss term l_e which describe the production and loss of free electrons in the plasma. These are local terms, which are related to chemical (and photochemical) reactions in the plasma. The term $\mathrm{div}(n_e \mathbf{u}_e)$ describes the effect of the movement of the electron fluid. This equation therefore allows us to identify the two effects that structure the ionosphere : chemical effects (which are dominant in the lower layers of the ionosphere, where the mean free path of particles is small compared to all other spatial scales), and transport effects (which are dominant at altitudes above approximately 300 km). In this section, we will focus on the former, and in the next section on the latter.

1.1 Photoionisation of the atmosphere

Photoionisation is the dominant process for electron production in the upper atmosphere, particularly at low latitudes (equatorial region). It is therefore the process we will study in this section, using a simplified model. However, it should be noted that other processes are involved and can have a significant impact on the observed plasma densities. The impact of energetic particles in particular, via the secondary emission mechanism, can play a role at high latitudes, close to the polar cones connected to the magnetosphere. The impacts of small solid bodies (meteors or shooting stars) also play a role in creating sporadic ionisation layers. At lower altitudes ($\sim$ 80 km), where solar ionising radiation has been almost completely absorbed, other sporadic phenomena (cosmic rays, solar X-ray bursts) can significantly alter the observed ionisation rates. The ionisation of the upper atmosphere is therefore the result of a variety of processes, but we will only study the main one here.

1.1.1 Zenith angle

To understand the distribution of ionisation zones, it is important to have an idea of the geometry of the Earth-Sun system, and in particular to introduce the concept of zenith angle.

A ray from the Sun reaches the Earth at an angle χ to the normal to the Earth's surface, where χ is the so-called zenith angle, which varies with the season and, of course, with the Earth's latitude and longitude (or rather the hour angle, or local time). Figure 1 shows the geometry of the system. In this figure, δ is the solar declination, i.e. the angle between the incident rays and the Earth's equator. This angle depends on the day

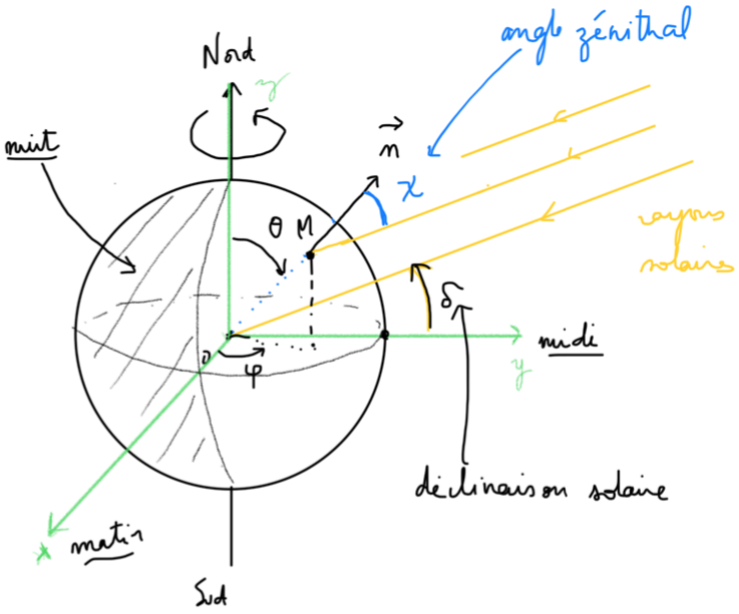

FIGURE 1 – Zenith angle between the direction of the sun's rays and the local vertical.

of the year, its minimum value being $\delta = 0$ at the equinoxes and its maximum value $\delta = \pm 23.44°$ at the solstices.

The unit vector $\mathbf{u}_{ray}$ along a solar ray can be expressed in the Cartesian coordinate system of Figure 1 as : $\mathbf{u}_{ray} = (0, -\cos\delta, -\sin\delta)$. The zenith angle is therefore such that

$$\cos\chi = -\mathbf{u}_{ray} \cdot \mathbf{n} \tag{2}$$

where $\mathbf{n}$ is the normal vector to the surface of the sphere at point $M(\theta, \phi)$ where we are seeking to calculate χ. This normal vector has coordinates in the Cartesian coordinate system $\mathbf{n} = (\sin\theta\cos\phi, \sin\theta\sin\phi, \cos\theta)$. We can deduce the expression of χ as a function of the coordinates (θ, ϕ) :

$$\cos\chi = \sin\delta\cos\theta + \cos\delta\sin\theta\sin\phi. \tag{3}$$

We often express χ in terms of the latitude $\theta_{lat} = \frac{\pi}{2} - \theta$ and the local hour angle counted from midnight $H = \phi + \frac{\pi}{2}$. In terms of these angles, we have

$$\cos\chi = \sin\delta\sin\theta_{lat} - \cos\delta\cos\theta_{lat}\cos H. \tag{4}$$

Figure 2 shows the distribution of the value of $\cos\chi$ on the Earth's sphere. We can see that the rays are more grazing at high latitudes and in the morning and evening, obviously. This figure reproduces fairly well the distribution of the ionisation level observed in the upper atmosphere, which, as we shall see, is proportional to $\cos\chi$.

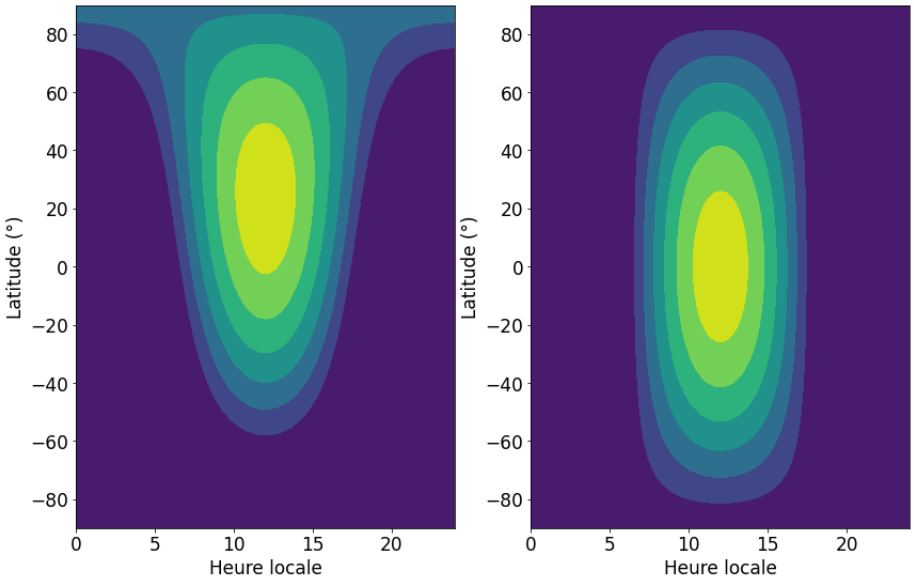

FIGURE 2 – Cosine of the zenith angle χ calculated at different points on the Earth's sphere during the summer solstice ($\delta = 23.44°$, left) and an equinox ($\delta = 0$, right)

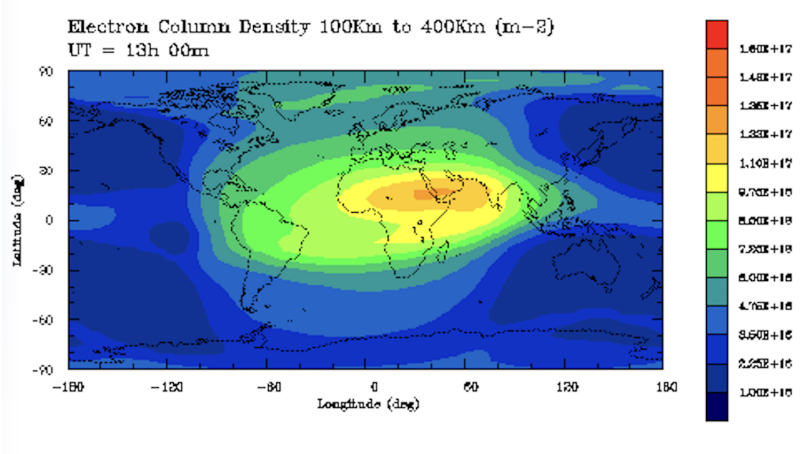

FIGURE 3 – TEC (total electron content) of the ionosphere in a longitude-latitude projection.

1.1.2 Optical thickness of the atmosphere

Consider the interaction of a solar ray with the Earth's atmosphere. As we have just seen, the ray arrives on Earth at an angle of incidence χ relative to the normal. We consider the solar ray to be monochromatic, characterised by a photon flux density N_ν [$\mathrm{m}^{-2}.\mathrm{s}^{-1}$], and that the atmosphere is composed of a single atomic or molecular species, with density $n_n(z)$ (the index n referring to the density of *neutrals*, to avoid confusion later with the density of the plasma).

If the energy $h\nu$ of the photon is greater than the ionisation energy of the atom $W \sim 10$ eV, i.e. if its wavelength is smaller than $\lambda < hc/W \sim 100$ nm (we are therefore in the UV range), it will have a non-negligible probability of ionising the atom or molecule in question. This probability is characterised by a cross section, known as the photoionisation cross section, σ_{ph}, which is a chemical property of the atom or molecule in question.

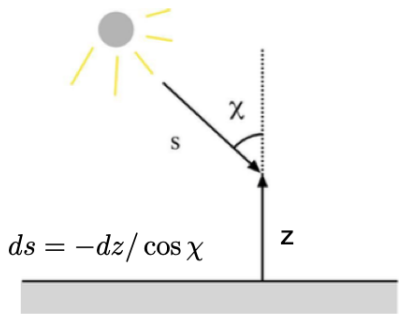

FIGURE 4 – Angle of incidence and relationship between ds and dz.

The probability that a photon will be absorbed when travelling a certain distance ds is (by definition of σ_{ph}) : $dp = \sigma_{ph} n_n ds = ds/\lambda_{ph}$. Where we can define $\lambda_{ph} = 1/(\sigma n_n)$ as the mean free path of the photon in the atmosphere.

The evolution of the photon current density is therefore given by

$$N_\nu(s + ds) = N_\nu(s)\,(1 - dp(s)) = N_\nu(s)\,(1 - \sigma_{ph} n_n ds) \tag{5}$$

This can be rewritten in the form of a differential equation (remember that $dz = -ds\cos\chi$, see fig.4) :

$$\frac{dN_\nu}{dz} = \frac{\sigma_{ph} n_n(z)}{\cos\chi} N_\nu(z). \tag{6}$$

which can be integrated as follows :

$$N_\nu(z) = N_\nu(\infty) \exp\left(-\frac{\sigma_{ph}}{\cos\chi}\int_z^\infty n_n(z)dz\right) \tag{7}$$

where $N_\nu(\infty)$ is the photon current density at infinity, before any interaction with the atmosphere (which is therefore a property of the light source, in this case the Sun).

The argument of the exponential in equation (7) is called the optical thickness $\tau(z)$ of the atmosphere at altitude z.

$$N_\nu(z) = N_\nu(\infty)e^{-\tau(z)}, \qquad \tau(z) = \frac{\sigma_{ph}}{\cos\chi}\int_z^\infty n_n(z)dz \tag{8}$$

The optical thickness $\tau(z)$ is a function of the wavelength of the incident radiation via σ_{ph} and, of course, the density of the atmosphere. $\tau(z) = 1$ gives the altitude at which the energy of the incident radiation has been divided by e.

The optical thickness of the entire atmosphere is by definition $\tau(0)$, if we place the origin of the z axis at the Earth's surface. It is a quantity that measures the transparency of the atmosphere at different wavelengths. Typically, $\tau(0) \ll 1$ in the visible wavelengths, while $\tau(0) \gg 1$ in the UV.

1.1.3 Photoelectron production rate

To obtain the electron production rate per unit volume q_e, we can now assume that the number of electrons dn_e produced (per unit area) between s and $s+ds$ is proportional to the number of photons absorbed (per unit area) between s and $s+ds$, i.e. to $-dN_\nu$. We therefore have $dn_e = -\eta dN_\nu$, where η is the average number of photoelectrons produced per absorbed photon. According to (6), we then have

$$q_e = \frac{dn_e}{ds} = -\eta\frac{dN_\nu}{ds} = \eta\sigma_{ph}n_n(z)N_\nu(z) \tag{9}$$

1.1.4 Case of an isothermal atmosphere

In the case of an isothermal atmosphere of temperature T, composed of a single species of atomic or molecular mass m, the density profile $n(z)$ is simply given by

$$n_n(z) = n_0 \exp\left(-\frac{z}{H}\right), \quad \text{where} \quad H = \frac{kT}{mg} \tag{10}$$

The optical thickness (8) can then be calculated simply, giving

$$\tau(z) = \frac{\sigma_{ph}n_0H}{\cos\chi}\exp\left(-\frac{z}{H}\right) = \tau(0)\exp\left(-\frac{z}{H}\right) \tag{11}$$

and therefore, according to (9)

$$q_e = \eta\sigma_{ph}n_0N_\nu(\infty)\exp\left(-\frac{z}{H} - \tau(0)\exp-\frac{z}{H}\right). \tag{12}$$

This is commonly referred to as the Chapman production function, named after Sydney Chapman, a pioneer in space plasma research (among other fields), who published this

result in 1930.

Note that we have calculated the production rate here assuming that the neutral density remains given by (10), which implies that our model is only valid if the ionospheric electron density is low compared to the neutral density : $n_e \ll n_n$ at all altitudes. If this condition is not met, a self-consistent model must be constructed in which $n_n(z)$ is itself a function of the production rate, but we will avoid this complication here.

The altitude z_m at which the ionisation rate is maximum can be easily found by taking the logarithmic derivative of (9) or (12),

$$z_m = H \ln \tau(0) = H \ln \frac{\sigma_{ph} H n_0}{\cos \chi} \tag{13}$$

where we can note that z_m corresponds to the height at which the optical depth is equal to 1 : $\tau(z_m) = 1$, i.e. the height at which the incident radiation is divided by e relative to its value at infinity. The maximum production rate q_{em} is

$$q_{em} = q_e(z_m) = \frac{\eta N_\nu(\infty) \cos \chi}{\exp(1) H}. \tag{14}$$

By introducing $y = (z - z_m)/H$, we can rewrite the production function in a more compact form, which is often found in the literature :

$$q_e = q_{em} \exp\left(1 - y - \exp(-y)\right) \tag{15}$$

1.2 Recombination processes

Now that we have quantified the electron creation rate, we need to evaluate the lifetime that a free electron can have before being recaptured by an ion, and which determines the loss term l_e in eq.(1). To do this we need to identify the dominant processes through which ions and electrons recombine.

1.2.1 Radiative recombination

Radiative recombination is the reverse reaction of photoionisation :

$$X + h\nu \rightleftarrows X^+ + e^- \tag{16}$$

The reaction cross section is σ_{ph} (the photoionisation cross section mentioned in the previous section), taken in the left-to-right direction, and σ_{rad}, the radiative recombination cross section, taken in the right-to-left direction.
The value of these cross sections obviously depends on the chemical nature of the compound X. The expressions for the cross sections are of the order of

$$\sigma_{ph} \sim 10^{-22}\ \mathrm{m}^2, \qquad \sigma_{rad} \sim 10^{-24}\ \mathrm{m}^2 \tag{17}$$

We can therefore see that the reaction is very unbalanced in the right-to-left direction. Radiative recombination is an inefficient process.

1.2.2 Dissociative recombination

In the presence of diatomic molecules, a more efficient recombination process exists,

$$XY^+ + e^- \rightarrow X^* + Y^* \tag{18}$$

whose cross section is given by

$$\sigma_{dis} \sim 10^{-18}\ \mathrm{m}^2, \tag{19}$$

i.e. a factor of 10^6 above σ_{rad}. It is therefore by far the dominant process in the presence of diatomic molecules, particularly in the lower layers of the atmosphere, via reactions on oxygen and nitrogen. It should be noted that energy conservation in this process generally leaves the atoms in an excited state. They de-excite by emitting photons, which are responsible for part of the phenomenon known as "airglow", limiting ground-based astronomical observations in the visible range.

1.2.3 Evaluation of electron density

We can now evaluate the electron density profile in the ionosphere using the continuity equation (1). To do this, we assume a static ionosphere ($\partial/\partial t = 0$) and neglect transport phenomena : $\mathbf{u}_e = 0$. The density is therefore given by the equality of the source and loss terms.

The temporal evolution of the electron concentration during a chemical recombination reaction of the type $A^+ + e^- \rightarrow A$, characterised by a cross section σ_{rec}, is given by

$$\frac{dn_e}{dt} = -l_e = -\sigma_{rec} v_{the} n_e n_{A^+} \tag{20}$$

where v_{the} is the thermal velocity of electrons, which is much higher than that of the ionic species. If we assume, as we have done so far, that the atmosphere consists of a single species, and that this species is ionised only once (which is reasonable if we assume that the electron density is very low compared to the neutral density $n_e \ll n$, an assumption already made to obtain the production rate in the previous section), then $n_{A^+} = n_e$, and the loss rate is proportional to the square of the electron density

$$l_e = \sigma_{rec} v_{the} n_e^2 \tag{21}$$

The electron density profile is then given by

$$n_e(z) = \sqrt{\frac{q_e(z)}{\sigma_{rec} v_{the}}} \tag{22}$$

1.3 Illustrations of the ionospheric structure

1.3.1 Isothermal model

To illustrate the results obtained, we consider a neutral atmosphere characterised by the following parameters :

$$\begin{cases} m = m_{N_2} \simeq 2.3 \times 10^{-26} \text{ kg} \\ T = 300K \\ p_0 = 1 \text{ bar} \end{cases} \tag{23}$$

These parameters correspond to a height scale $H \simeq 9$ km and a ground density $n_0 = p_0/kT \simeq 2.4 \times 10^{25}$ m^{-3}.

The density of *ionising* photons, i.e. in the UV range that interests us ($\lambda < 100nm$), arriving from the Sun at 1 AU is of the order of

$$N(\infty) \simeq 5 \times 10^{14} \text{ m}^{-2}\text{s}^{-1} \tag{24}$$

and we will take an ionisation number per photon $\eta = 1$. For the photoionisation/recombination cross sections, we take the values of σ_{ph} and σ_{dis} given in order of magnitude in the previous paragraph (dissociative recombination).

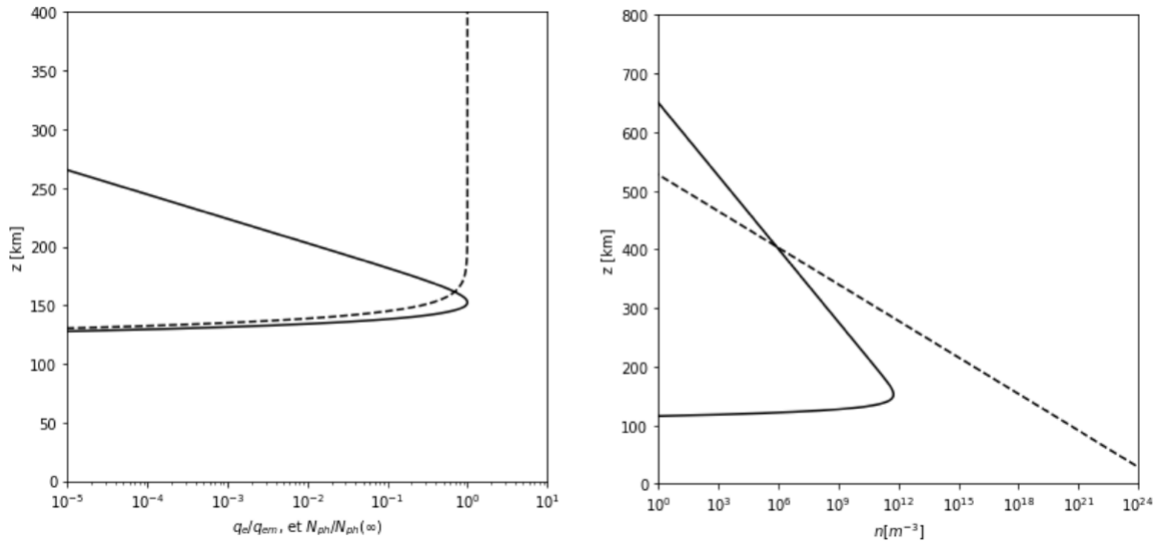

FIGURE 5 – Chapman layer for the N_2 atmosphere at 300 K described in the text. Left : Production rate (solid line) and photon current density (dotted line). Right : Neutral density (dotted line) and electron density (solid line).

The left part of Figure 6 shows the normalised values of the UV photon flux density and the production function q_e. The atmosphere at high altitudes is too sparse, and therefore too transparent, for the photoionisation process to be effective. Once they reach the denser layers, the photons are quickly absorbed, producing electrons locally. The production function therefore takes on non-negligible values in a layer around z_m, known as the Chapman layer.

The right-hand side of Figure 6 shows the values of the neutral density (dotted line) and electron density (solid line). Here again, we see the layered structure. It can be noted that while our model gives good results around the ionisation maximum, it no longer works at high altitudes (>350 km approximately), since the assumption $n_e \ll n_n$ is no longer valid there. At these altitudes, the plasma is highly ionised, the atmosphere is very sparse, and other effects (in particular diffusive transport) that are neglected here must be taken into account when modelling the plasma.

1.3.2 The layers of the Earth's ionosphere

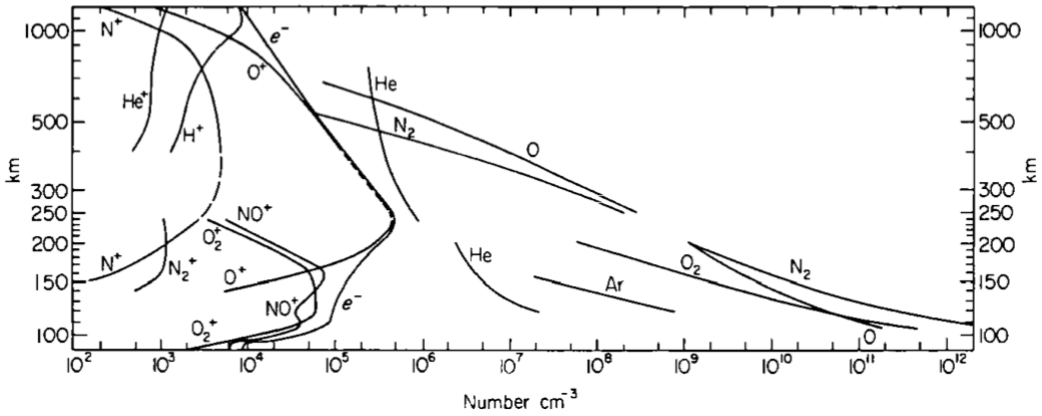

FIGURE 6 – Composition of the neutral atmosphere and ionosphere as a function of altitude. Measurements from sounding rockets (daytime, White Sands, New Mexico) for altitudes below 250 km. Measurements from the Elektron II satellite above 250 km.

In this section, in order to understand and model the process of ionosphere generation, we have considered the simple model of an atmosphere with a single chemical component ionised by monochromatic radiation. The reality is obviously more complex, as the atmosphere is composed of multiple chemical species, each characterised by an ionisation cross section acting at different wavelengths. All these effects are modelled using numerical models.

However, it is understandable that, since the scale height H is a function of particle mass, the heaviest molecules will be found at the lowest altitudes. And the higher the

altitude, the greater the proportion of light molecules and atoms. Gravity therefore produces a stratification of chemical elements, which has an effect on the structure of the ionosphere.

The ionospheric layers are designated by letters and, from bottom to top, are characterised by :

— Layer D (altitude 70-90 km) : mainly composed of NO^+ and O_2^+, present only during the day, its ionisation rate is a fairly important function of solar activity (production by hard solar X-ray bursts).

— E layer (peak density altitude around 110 km) : O_2^+ is predominant, its density drops just after sunset to its "night-time" equilibrium value. This layer therefore remains present at night. Produced mainly by the absorption of the UV continuum, as well as by hydrogen lines (Lyman beta) and X-rays.

— Layer F1 (around 200 km), O^+ predominant, disappears completely during the night. Produced mainly by the absorption of the UV continuum (10-80 nm), as well as He II lines.

— Layer F2 (around 300 km), O^+, N^+ persists during the night. Produced mainly by the absorption of the UV continuum (10-80 nm), as well as He II lines.

2 Transport phenomena

In the previous section, we focused on chemical reactions, which are local in nature, neglecting the term for electron (or ion) transport. In this section, we will focus on the latter.

2.1 Mobility and diffusion in a magnetised plasma

Here we will study the response of a partially ionised plasma to the application of constant external forces. We denote by $\nu_{i,e}$ the collision frequencies between ions and neutrals (index i) or between electrons and neutrals (index e). These collision frequencies are given by

$$\nu_\alpha = n_n \sigma_c v_{th\alpha} \tag{25}$$

where n_n is the neutral density, σ_c is the cross section for collisions with neutrals (of the same order of magnitude for ions and electrons) and $v_{th\alpha} = (kT_\alpha/m_\alpha)^{1/2}$ is the thermal velocity.
To keep the problem reasonably simple, we will consider the collision frequencies between ions and electrons to be negligible, the temperatures to be constant (independent of

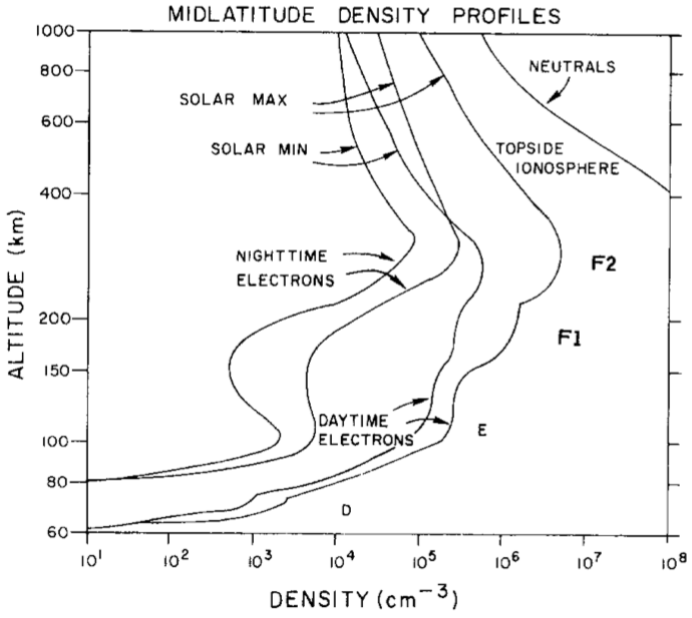

FIGURE 7 – Electron density at mid-latitudes as a function of altitude, showing the layered structure, its variability between day and night, and with the solar cycle.

position), and the plasma to consist of a single atomic or molecular species, ionised only once. The fundamental equation of dynamics is written as

$$0 = n_\alpha m_\alpha \mathbf{g} - kT_\alpha \nabla n_\alpha + n_\alpha q_\alpha (\mathbf{E} + \mathbf{u}_\alpha \times \mathbf{B}) - n_\alpha m_\alpha \nu_\alpha (\mathbf{u}_\alpha - \mathbf{U}) \tag{26}$$

where $\alpha = i, e$. $\mathbf{g}$ is the acceleration due to gravity, $\mathbf{E}$ is the electric field, $\mathbf{B}$ is the magnetic field, and $\mathbf{U}$ represents a possible velocity relative to the observation reference frame (generally linked to the Earth's surface). This velocity can play an essential role in ionospheric electrodynamic phenomena, which are often generated by neutral winds, whose velocities are significant (> 100 m/s) in the thermosphere.

In this equation, we have neglected the inertial term $\mathbf{u} \cdot \nabla \mathbf{u}$ as compared to the viscosity term $\nu \mathbf{u}$. This is possible for a subsonic and collisional fluid (low Knudsen number). Indeed, we can see that (introducing L as the typical spatial dimension of the system)

$$\frac{|\mathbf{u} \cdot \nabla \mathbf{u}|}{|\nu \mathbf{u}|} \sim \frac{u}{\nu L} \sim \frac{u/v_{th}}{L/\ell_{lpm}} \sim M_a K_n \tag{27}$$

where M_a is the Mach number and K_n is the Knudsen number.

In order to simplify and eliminate the explicit dependence on $\mathbf{U}$, we reformulate the equation of dynamics in the reference frame in which the neutrals are at rest :

$$0 = n_\alpha m_\alpha \mathbf{g} - kT_\alpha \nabla n_\alpha + n_\alpha q_\alpha (\mathbf{E'} + \mathbf{u'}_\alpha \times \mathbf{B}) - n_\alpha m_\alpha \nu_\alpha \mathbf{u'}_\alpha \tag{28}$$

where $\mathbf{u'}_\alpha = \mathbf{u}_\alpha - \mathbf{U}$ and $\mathbf{E'} = \mathbf{E} + \mathbf{U} \times \mathbf{B}$, for a non-relativistic change of reference frame.

We can express the velocity $\mathbf{u'}_\alpha$:

$$\mathbf{u'}_\alpha - \kappa_\alpha \mathbf{u'}_\alpha \times \mathbf{b} = \mu_\alpha (m_\alpha \mathbf{g} + q_\alpha \mathbf{E'}) - D_\alpha \frac{\nabla n_\alpha}{n_\alpha} = \mathbf{w}_\alpha \tag{29}$$

Where we have introduced the mobility coefficients of species α : $\mu_\alpha = 1/(m_\alpha \nu_\alpha)$ and the diffusion coefficient $D_\alpha = kT_\alpha/(m_\alpha \nu_\alpha) = kT_\alpha \mu_\alpha$. $\kappa_\alpha = q_\alpha B/(m_\alpha \nu_\alpha)$ is the ratio of the cyclotron frequency of population α to its collision frequency with neutrals (note that $\kappa_e < 0$ with this definition). $\mathbf{w}_\alpha$ is the velocity that population α would have in the absence of a magnetic field.

Equation (29) allows us to discuss the limiting cases of a weak field $\kappa_\alpha \ll 1$ and a strong field $\kappa_\alpha \gg 1$.

In the first case, $\kappa_\alpha \ll 1$, we see that $\mathbf{u'}_\alpha \simeq \mathbf{w}_\alpha$, so everything behaves as if there were no magnetic field : charged particles move through a population of neutral particles with which they collide : apart from the diffusion effect, their average velocity is therefore proportional to the forces applied (Ohm's effect or similar), the work done by the forces that cause them to move being transmitted to the neutral particles in the form of heat (Joule effect or similar).

In the second case, $\kappa_\alpha \gg 1$, we then have $\kappa_\alpha \mathbf{u'}_\alpha \times \mathbf{b} \simeq -\mathbf{w}_\alpha$, and therefore

$$\mathbf{u'}_{\perp\alpha} \simeq \frac{\mathbf{w}_\alpha}{\kappa_\alpha} \times \mathbf{b} \simeq \frac{1}{q_\alpha B^2} (m_\alpha \mathbf{g} + q_\alpha \mathbf{E'} - kT_\alpha \frac{\nabla n_\alpha}{n_\alpha}) \times \mathbf{B} = \mathbf{V}_g + \mathbf{V}_\times + \mathbf{V}_{dm}. \tag{30}$$

where $\mathbf{u'}_{\perp\alpha}$ is the perpendicular component of the velocity of population α, $\mathbf{u'}_{\perp\alpha} \equiv \mathbf{u'}_\alpha - (\mathbf{u'}_\alpha \cdot \mathbf{b})\mathbf{b}$. The component of the velocity parallel to the magnetic field is, of course, the solution to the "no magnetic field" equation discussed above.

Since collisions occur very slowly compared to the cyclotron frequency, we find magnetic drift motions perpendicular to both the applied force and the magnetic field. The three terms on the right-hand side are, in order of appearance : the gravitational drift velocity, the cross-field drift velocity, and the diamagnetic drift velocity.

What happens in an intermediate case ? We can imagine that the velocity of the particles will then have two components : an "Ohmic" component parallel to the applied forces and a "magnetic drift" component perpendicular to both these forces and the magnetic field.
To answer this question, we can solve equation (29), for example by reformulating it as an algebraic system (we temporarily omit the indices α) :

$$\begin{cases} u'_x - \kappa u'_y = w_x \\ \kappa u'_x + u'_y = w_y \\ u'_z = w_z \end{cases} \tag{31}$$

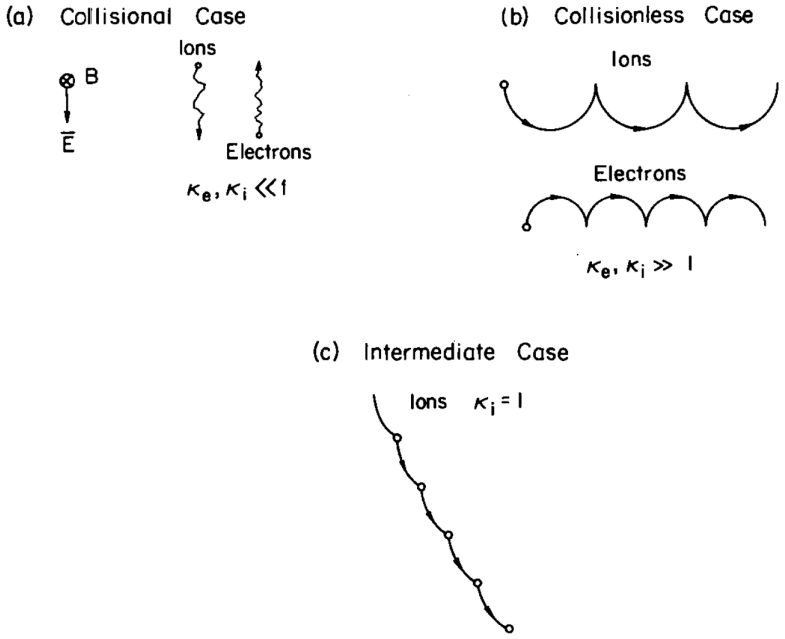

FIGURE 8 – Schematic particle trajectories for the limiting cases $\kappa \ll 1$, $\kappa \gg 1$, $\kappa \sim 1$. Only the electric force is taken into account in this figure.

Where we have taken the z axis of our coordinate system parallel to the magnetic field. The system is written in matrix form $\mathbf{w} = A \cdot \mathbf{u'}$, and is solved by inverting the matrix A :

$$\begin{pmatrix} u'_x \\ u'_y \\ u'_z \end{pmatrix} = \begin{pmatrix} \frac{1}{1+\kappa^2} & \frac{\kappa}{1+\kappa^2} & 0 \\ -\frac{\kappa}{1+\kappa^2} & \frac{1}{1+\kappa^2} & 0 \\ 0 & 0 & 1 \end{pmatrix} \begin{pmatrix} w_x \\ w_y \\ w_z \end{pmatrix} \tag{32}$$

We can therefore see that the mobility and diffusion coefficients take different values depending on the direction considered. In the direction of the magnetic field, they remain unchanged, and we have

$$u'_{\alpha z} = \mu_\alpha (m_\alpha g_z + q_\alpha E'_z) - \frac{D_\alpha}{n_\alpha} \frac{dn_\alpha}{dz} \tag{33}$$

In the plane perpendicular to the magnetic field, we must separate the direction of the forces (or density gradient), along which we have a mobility, or effective diffusion coefficient, equal to

$$\mu_{P\alpha} = \frac{\mu_\alpha}{1+\kappa_\alpha^2} \qquad D_{P\alpha} = kT_\alpha \mu_{P\alpha} = \frac{D_\alpha}{1+\kappa_\alpha^2} \tag{34}$$

and the direction perpendicular to both the forces and the magnetic field, along which

there is mobility or an effective diffusion coefficient equal to

$$\mu_{H\alpha} = \frac{\kappa_\alpha \mu_\alpha}{1+\kappa_\alpha^2} \qquad D_{H\alpha} = kT_\alpha \mu_{H\alpha} = \frac{\kappa_\alpha D_\alpha}{1+\kappa_\alpha^2}. \tag{35}$$

The indices P and H refer to *Pedersen* and *Hall*.

2.1.1 Expression of the conductivity

We discussed the general case of mobilities in the previous section, but it is interesting to look at the special case of the electric field, which is often the dominant term.

The conductivity σ of the plasma is defined by $\mathbf{j} = \sigma \cdot \mathbf{E}$, where $\mathbf{j} = e(n_i \mathbf{u}_i - n_e \mathbf{u}_e)$, if we consider that the ionic species is simply ionised. To simplify the expressions, we assume in what follows that the plasma is quasi-neutral, i.e. that $n_e = n_i = n$. The conductivity matrix can therefore be expressed simply from the mobility matrix (32),

$$\sigma = \begin{pmatrix} \sigma_P & -\sigma_H & 0 \\ \sigma_H & \sigma_P & 0 \\ 0 & 0 & \sigma_0 \end{pmatrix} \tag{36}$$

where the matrix elements are given by (note the $-$ sign in the definition of σ_H, which we have introduced so that the conductivity is positive, see below).

$$\begin{cases} \sigma_0 = ne^2 \left(\mu_i + \mu_e\right) \\ \sigma_P = ne^2 \left(\frac{\mu_i}{1+\kappa_i^2} + \frac{\mu_e}{1+\kappa_e^2}\right) \\ \sigma_H = -ne^2 \left(\frac{\kappa_i \mu_i}{1+\kappa_i^2} + \frac{\kappa_e \mu_e}{1+\kappa_e^2}\right) \end{cases} \tag{37}$$

where, again, by specifying the masses and charges of the particles :

$$\begin{cases} \sigma_0 = \frac{ne^2}{m_i \nu_i} + \frac{ne^2}{m_e \nu_e} \\ \sigma_P = \frac{ne^2}{m_i \nu_i} \frac{1}{1+\kappa_i^2} + \frac{ne^2}{m_e \nu_e} \frac{1}{1+\kappa_e^2} \\ \sigma_H = \frac{ne}{B} \left(\frac{\kappa_e^2}{1+\kappa_e^2} - \frac{\kappa_i^2}{1+\kappa_i^2}\right) \end{cases} \tag{38}$$

The expression for σ_0, the conductivity in the direction parallel to the magnetic field, is identical to that which we would have in a non-magnetised plasma. It is dominated by the electronic term, since, using (25), the ratio of electrons to ions is $m_i \nu_i / m_e \nu_e = (m_i/m_e)^{1/2} (T_i/T_e)^{1/2} \sim 40$. We therefore have, with good accuracy, $\sigma_0 \simeq \frac{ne^2}{m_e \nu_e}$.

The values of the Pedersen and Hall terms depend on the ratio κ of the gyrofrequency to the collision frequency, which in the ionosphere is a function of altitude, mainly due to the variation in neutral density with altitude (and therefore the decrease in ν) as we will see in the following paragraph.

2.1.2 Order of magnitude of mobilities and conductivities in an isothermal atmosphere

To identify the dominant processes at different altitudes, we return to the simplified isothermal atmosphere model presented in Section 1. The neutral density therefore decreases with altitude according to an exponential law characterised by a height scale $H = kT/mg$. The parameters used to characterise the neutral atmosphere are the same as those in section 1.3.1.

To obtain the values of mobility and conductivity, a magnetic field model is also required : the Earth's field is globally dipolar, $B(r) = B_T(r/R_T)^3$ where $B_T \simeq 0.5$ G (1 G $\equiv 10^{-4}$ T). For low altitudes ($z - R_T \ll R_T$), we therefore have $B(z) \simeq B_T(1 - 3z/R_T)$. We can therefore see that if we consider an atmospheric layer of a few hundred kilometres, we can safely assume that the field is constant (the relative error made on B being of the order of $3\Delta z/R_T \sim 10$ % for $\Delta z = 200$ km). We will therefore assume a constant field $B = 0.5$ G, which does not qualitatively change the results and avoids adding too many ingredients to the model.

Fig. 9 shows the evolution of the three components of electron mobility. We can see that the parallel mobility $\mu_{e,0}$ increases exponentially with altitude, since the electron-neutral collision frequency is inversely proportional to the neutral density $\nu_e \propto 1/n$, and $n \propto \exp(-z/H)$.

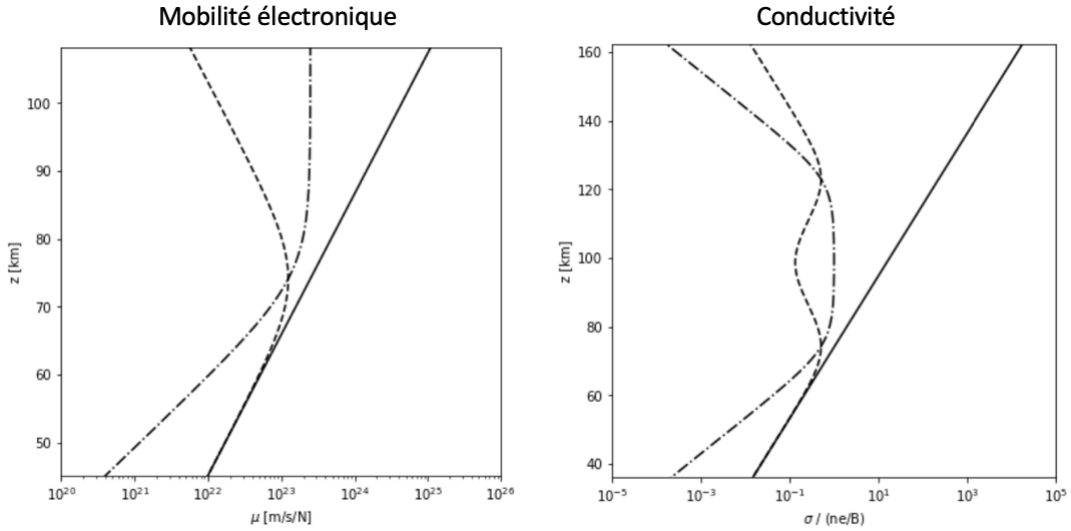

FIGURE 9 – Variation with altitude of electron mobilities μ_e (–), $\mu_{e,P}$ (- -) and $\mu_{e,H}$ (-.-) (left figure) and conductivities σ (–), σ_P (- -) and σ_H (-.-) normalised by ne/B (right-hand figure) in an isothermal atmosphere of N_2 at 300 K (see text for parameters).

The Pedersen mobility $\mu_{e,P}$ is initially confused with $\mu_{e,0}$ since, for the lower layers of the atmosphere, $\kappa_e \ll 1$: the plasma is highly collisional and the magnetic field has no effect on mobility. Then, at the altitude where the gyrofrequency is of the order of the collision frequency (approximately 70 km for electrons, approximately 120 km for ions), the two curves separate, and the conductivity perpendicular to the B field decreases as κ_e increases.

The Hall mobility $\mu_{e,H}$ (which, recall, is proportional to $\kappa/(\kappa^2+1)$) is low at low altitudes and increases with altitude, until it becomes the dominant perpendicular term at high altitudes, when collisions become infrequent ($\kappa \gg 1$) and the movement of electrons is effectively comparable to their magnetic drift (the mobility μ then becomes constant since the velocity of the particles is $\mathbf{w} = \mathbf{F} \times \mathbf{B}/B^2$, which is independent of altitude in our model since the modulus of $\mathbf{B}$ is considered constant).

Fig. 9 also shows the evolution of conductivity (normalised by en/B) with altitude. As we have seen, parallel conductivity is dominated by the mobility of electrons, which is much greater than that of ions. It is therefore approximately equal to $ne^2/m_e\nu_e$ and increases exponentially with altitude.

Pedersen conductivity (in the direction parallel to $\mathbf{E}$ and perpendicular to $\mathbf{B}$) has two maxima. The first is around 70 km, linked to the maximum of $\mu_{e,P}$: at this altitude, the current is carried by electrons (for which $\kappa_e \sim 1$), while the ions are still highly collisional ($\kappa_i \ll 1$). The second maximum occurs at around 130 km altitude, linked to the maximum of $\mu_{i,P}$, for which the current is mainly carried by ions ($\kappa_i \sim 1$) while the electrons are highly magnetised ($\kappa_e \gg 1$) and move mainly via their drift motion in cross fields in the direction perpendicular to $\mathbf{E}$.

Hall conductivity is low at low altitudes (the plasma is not magnetised, $\kappa_e \ll 1$ and $\kappa_i \ll 1$). It becomes dominant between 80 and 120 km altitude, in the zone where electrons are magnetised ($\kappa_e \gg 1$) while ions are not ($\kappa_i \ll 1$) : electrons move with their drift motion, which is not the case for ions, which are collisional, hence the existence of a net current in the direction perpendicular to both $\mathbf{E}$ and $\mathbf{B}$.

At high altitude, both the ion and electron populations are relatively non-collisional ($\kappa_e \gg 1$ and $\kappa_i \gg 1$). The two populations therefore move according to their drift in crossed fields, whose speed is independent of charge and mass. The two populations are therefore driven by the same motion, and the current, resulting from the difference in speed between electrons and ions, therefore tends towards zero as altitude increases.

To conclude this section, it is interesting to note that the conductivity perpendicular to the magnetic field takes on non-negligible values in a layer several tens of kilometres thick (around the ionospheric E region). The altitude of this layer is determined by the zone where the collision frequency between charged and neutral particles is of the order of the gyrofrequency of electrons or ions. The fact that this altitude corresponds precisely to the altitude of the ionisation layer (Chapman layer), i.e. the altitude where there are a significant number of charged particles to carry the current, is a coincidence (the value of the Earth's magnetic field amplitude, which determines the cyclotron frequency, has no a priori reason to be correlated with the parameters that determine the collision frequency

and the altitude of the Chapman layer, i.e. the density of the Earth's atmosphere and solar irradiance). This coincidence, which is responsible for multiple electrodynamic phenomena in the ionosphere (which we will return to below), will therefore not necessarily be found in studies of other planetary ionospheres, or even in studies of the Earth's ionosphere at times other than our own (as the Earth's magnetic field and solar irradiance vary significantly over long time scales).

2.2 Some effects of ionospheric transport

2.2.1 Ambipolar diffusion and plasma height scale

In order to calculate the typical height scale of ionised species (electrons and ions) and show that it is different from that of neutral species, we return to expression (29) for the velocity of electronic and ionic species (index $\alpha = \mathrm{e}, \mathrm{i}$). We limit ourselves to the vertical component (i.e. parallel to the acceleration due to gravity $\mathbf{g}$) of the velocity and consider a non-magnetised case (or one in which the magnetic field lines are vertical). We also consider that the neutrals are at rest relative to the plasma. We then have, projecting along an axis (Oz) directed upwards,

$$\begin{cases} \mu_e^{-1} w_e = -m_e g - eE_z - \frac{kT_e}{n_e}\frac{\partial n_e}{\partial z} \\ \mu_i^{-1} w_p = -m_i g + eE_z - \frac{kT_i}{n_i}\frac{\partial n_i}{\partial z} \end{cases} \tag{39}$$

We further assume that $n_e \simeq n_i \simeq n$ (electro-neutrality) and that $w_e \simeq w_i \simeq w$ (absence of vertical current). We can eliminate the electric field by adding these two equations and express the average velocity w of the plasma as

$$\left(\frac{1}{\mu_e} + \frac{1}{\mu_i}\right) w = -(m_e + m_i)g - \frac{k(T_e + T_i)}{n}\frac{\partial n}{\partial z} \tag{40}$$

The ratio of the mobility coefficients is

$$\frac{\mu_e}{\mu_i} = \frac{m_i \nu_i}{m_e \nu_e} \propto \sqrt{m_i/m_e} \gg 1, \tag{41}$$

we see that we can therefore neglect the term in $1/\mu_e$ in front of the term in $1/\mu_i$. Neglecting m_e in front of m_i in the same way, we finally obtain

$$w = -\mu_i m_i g - \frac{D_{ap}}{n}\frac{\partial n}{\partial z} = \frac{1}{\nu_i}\left(-g - \frac{k(T_e + T_i)}{n m_i}\frac{\partial n}{\partial z}\right) \tag{42}$$

where D_{ap} is the so-called *ambipolar* diffusion coefficient,

$$D_{ap} = \mu_i k(T_e + T_i) = \frac{k(T_e + T_i)}{m_i \nu_i}. \tag{43}$$

The continuity equation for plasma, $\partial_t n + \text{div}\, n\mathbf{w} = 0$, allows us to express the evolution of density in the form

$$\frac{\partial n}{\partial t} + \frac{\partial}{\partial z}\left(-n\mu_i m_i g - D_{ap}\frac{\partial n}{\partial z}\right) = 0 \tag{44}$$

which is a Fokker-Planck equation describing the evolution of plasma density via a convection term (first term, proportional to the applied force, here $m_i g$) and a diffusion term (second term), with a coefficient D_{ap}. It is interesting to note that while convection occurs as if the fluid were composed solely of protons (electron parameters do not come into play), ambipolar diffusion involves electron temperature. We can see that the presence of electrons increases the diffusion coefficient—by a factor of 2 if the electron and ion temperatures are of the same order, and more if $T_e > T_i$, which is generally the case.

The gravitational height scale of the plasma is determined by the equilibrium between convection and diffusion effects. It is obtained by seeking a stationary solution to equation (44). This must satisfy

$$n\mu_i m_i g + D_{ap}\frac{dn}{dz} = 0, \tag{45}$$

and we obtain a plasma density of the form

$$n(z) = n_0 \exp\left(-\frac{\mu_i m_i g z}{D_{ap}}\right) = n_0 \exp\left(-\frac{m_i g z}{k(T_e + T_i)}\right). \tag{46}$$

We again find an exponentially stratified atmosphere, but the height scale is $H_{ap} = k(T_e + T_i)/m_i g$, which is therefore larger (by a factor of about 2 if $T_e \simeq T_i$) than that of a neutral fluid.

This can be understood as follows : electrons, which are lighter, are much more mobile than ions. If the ion and electron gases behaved independently of each other, the electron gas would therefore have a much larger ($\sim$ 2000 times larger) height scale than the ion gas. Such a situation would create a high volume charge and a strong electric field. This field, directed from bottom to top, would have the effect of pulling the electrons back to the ground and decreasing their height scale, and conversely pulling the ions upwards, increasing their height scale. The assumption of electroneutrality that we have imposed reflects the existence of this *ambipolar* electric field E_{ap} which ensures the cohesion of the electron and ion populations.

We can calculate E_{ap} using one of the equations (39) in the stationary case ($w = 0$). We obtain

$$eE_{ap} = \frac{T_e}{T_e + T_i} m_i g \tag{47}$$

It may be interesting to look at the effective force experienced by an ion or an electron in the gravitational field and the ambipolar field. For an ion, we have

$$F_i = -m_i g + eE = -m_i g\left(1 - \frac{T_e}{T_e + T_i}\right) \simeq -\frac{m_i g}{2} \tag{48}$$

and for an electron

$$F_e = -m_e g - eE \simeq -m_i g \frac{T_e}{T_e + T_i} \simeq -\frac{m_i g}{2} \tag{49}$$

where the evaluations of the last member are for $T_e \simeq T_i$. Thus, the effect of the electric field is to decrease the effective mass of the ions by a factor of 2 and to give the electrons an effective mass $m_i/2$, so that the two populations have the same height scale, which is necessary to maintain electro-neutrality in the plasma.

2.2.2 Electrodynamics of low latitudes : dynamo effect, Sq current system and equatorial electrojet

The atmospheric dynamo effect was proposed as early as 1882 by Balfour Stewart, a Scottish physicist who was interested in terrestrial magnetism and had noticed significant daily variations in the horizontal component of the geomagnetic field, with periods equal to fractions of 24 hours (solar day) and 24.8 hours (lunar day). The (simplified) theory presented here was developed much later, in the 1960s.

The dynamo effect proceeds in the following stages :

— Strong atmospheric winds, mainly in the west → east direction, are generated in the thermosphere (at an altitude of approximately 100 km) by the effects of lunar and solar tides, as well as thermal effects related to the difference in temperature between day and night.

— These winds carry with them, through viscosity (collisions), the charged particles of the ionosphere, forcing them to move perpendicular to the Earth's magnetic field. They carry ions (strongly collisionally coupled to neutrals at this altitude, $\kappa_i \ll 1$) more easily than electrons (highly magnetised at this altitude, $\kappa_e \gg 1$).

— This results in an electric current perpendicular to the field $\mathbf{B}$ and the wind speed $\mathbf{U}$, and therefore essentially vertical. However, the vertical dimension of the conductive layer is finite (see fig.9) : the current cannot move freely, and electric charges will accumulate at the boundaries of the conduction layer.

— The polarisation of the conduction layer creates an electric potential field which in turn modifies the current distribution, so that the divergence of the current distribution is zero and a steady-state equilibrium can be established.

The transport equations we derived in the previous section allow us to model these effects. We consider that there is a movement of neutrals relative to the Earth's surface, with a velocity $\mathbf{U}$. The expression for the current density is given by

$$\mathbf{j} = \sigma \cdot \mathbf{E'} = \sigma \cdot (\mathbf{U} \times \mathbf{B} - \nabla\Phi) \tag{50}$$

where $\mathbf{U} \times \mathbf{B}$ is the electromotive field and $\nabla\Phi$ is the electric field due to the presence of polarisation charges. σ is the conductivity matrix that we derived in the previous section.

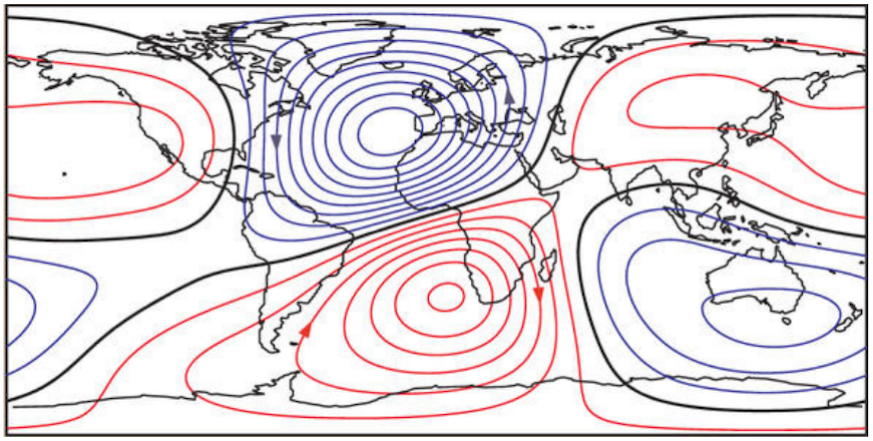

FIGURE 10 – Sq current system : ionospheric current lines derived from data taken at the Huancayo Observatory in Peru. Increments of 10 kA between two successive lines. The blue lines rotate counterclockwise and the red lines clockwise. The area of very strong West → East currents at the diurnal equator is the *equatorial electrojet*.

We seek to describe the ionospheric current system that establishes itself in a steady state. Charge conservation is written as $\partial_t \rho + \text{div } \mathbf{j} = 0$, which implies that the divergence of the current must be zero in such an equilibrium,

$$\text{div } [\sigma \cdot (\mathbf{U} \times \mathbf{B} - \nabla \Phi)] = 0 \tag{51}$$

We can see that the current field will reflect the (generally complex) shape of the wind velocity field that is its source, as well as the conductivity structure via σ, and the temporal variations (day/night for σ, related to tidal effects for $\mathbf{U}$) of these parameters. We are therefore dealing with a fairly complex structure, which we refer to as the *current system Sq*. Sq refers to *Solar quiet*, insofar as this current system is established in the absence of intense magnetic activity of solar origin.

To simplify the problem (and because this is where the dynamo is most effective), we consider areas close to the Earth's equator. We choose a coordinate system (x, y, z) such that x points upwards, y points eastwards and z points northwards. In this coordinate system, we have $\mathbf{U} = U.\mathbf{u}_y$ and $\mathbf{B} = B.\mathbf{u}_z$. We consider a slice geometry, in which conductivity is non-zero only in a slice of altitudes. Fig. **??** shows the geometry of the problem.

The current in the x direction is, according to (50),

$$j_x = \sigma_P E'_x - \sigma_H E'_y = \sigma_P \left(UB - \frac{\partial \Phi}{\partial x} \right) + \sigma_H \frac{\partial \Phi}{\partial y} = 0 \tag{52}$$

since in steady state there can be no net current in this direction. This relationship allows

us to link the *zonal* electric field (i.e. in the west-east direction) to the vertical field

$$E'_x = UB - \frac{\partial \Phi}{\partial x} = -\frac{\sigma_H}{\sigma_P}\frac{\partial \Phi}{\partial y} \tag{53}$$

This expression allows us to obtain the zonal current, since we know that

$$j_y = \sigma_H E'_x + \sigma_P E'_y = -\sigma_P \left(1 + \frac{\sigma_H^2}{\sigma_P^2}\right) \frac{\partial \Phi}{\partial y} \tag{54}$$

where $\sigma_C = \sigma_P(1 + \sigma_H^2/\sigma_P^2)$ is called Cowling's conductivity. We can see that the effect of charge accumulation at the boundaries of the conductive zone (represented by the assumption $j_x = 0$) increases the conductivity in the zonal direction by a factor of $(1 + \sigma_H^2/\sigma_P^2) \sim 100$ in layer E. This increase in conductivity is the source of the strong ionospheric current called the equatorial electrojet (see fig.10).

The Sq current system, and in particular the strong equatorial electrojet, is responsible for the daily disturbances in the magnetic field, as Balfour Stewart had hypothesised. These variations are illustrated in Figure 11. In practice, given the difficulties in measuring the electric field or ionospheric currents in situ, it is these magnetic field measurements that are currently used to infer the distribution of the current system.

2.2.3 Electrodynamics of high latitudes : couplings to the solar wind and the magnetosphere

At high latitudes, the geomagnetic field lines are (as a first approximation) vertical. They extend to very high altitudes and connect the ionosphere to the magnetosphere or directly to the interplanetary medium. This connection results in a number of specific effects, in particular a system of ionospheric currents generated by the electromotive fields of the solar wind and the magnetosphere, which is therefore different from the Sq system observed at low and middle latitudes.

The ionosphere at high latitudes is divided into two regions. Region I is the region of highest magnetic latitude, also known as the polar cap, where the Earth's magnetic field lines are directly connected to the solar wind. Region II is the region of lower latitudes, where the magnetic field lines connect the ionosphere to the inner magnetosphere. We will see that ionospheric currents flow in opposite directions in these two regions (and therefore cancel each other out at the boundary between them).

Fig. 12 illustrates the connection in region I between the solar wind and the ionosphere. The magnetic field lines, which are highly conductive, can be considered isopotential, meaning that they project the interplanetary electric field onto the ionospheric surface. This system can be thought of as an electrical circuit in which the solar wind's induction field acts as a generator, the magnetic field lines act as electrical cables, and the ionosphere acts as a resistor.

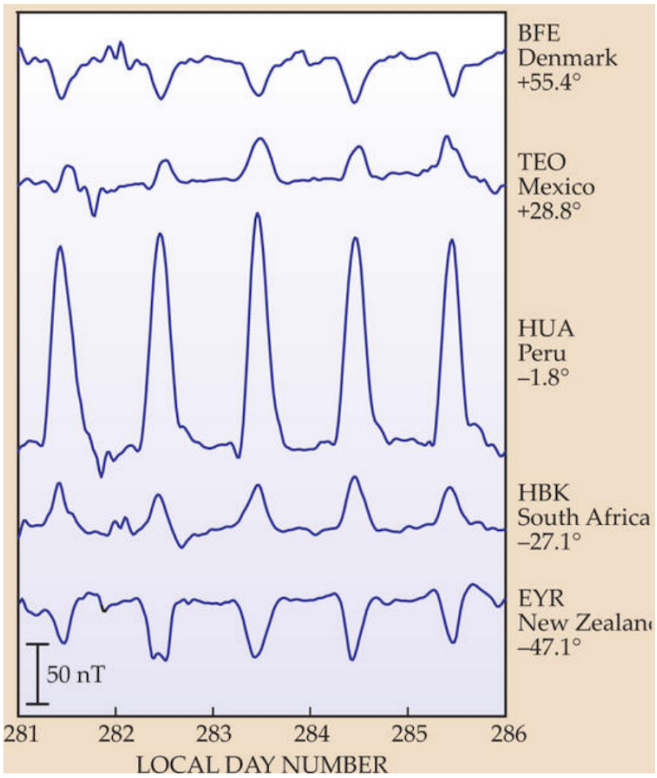

FIGURE 11 – Disturbances in the Earth's magnetic field measured by five observatories located at different magnetic latitudes between 8 and 12 October 2003. Note the polarity reversal between low and high latitudes.

We can attempt to evaluate the power (per unit volume) injected into this circuit. This is equal to $\mathcal{P} = -\mathbf{J}_{sw} \cdot \mathbf{E}_{sw}$. The current $\mathbf{J}_{sw}$ flowing in the circuit is related to the dynamics of the solar wind plasma by

$$\rho \frac{d\mathbf{U}_{sw}}{dt} = -\nabla p + \mathbf{J}_{sw} \times \mathbf{B}. \tag{55}$$

where $\rho \simeq n_{sw} m_p$ is the density of the solar wind. The current $\mathbf{J}_{\perp,sw}$ flowing between two field lines is obtained by taking the vector product of this equation with $\mathbf{B}$ and dividing by B^2,

$$\mathbf{J}_{\perp,sw} = \frac{1}{B^2} \left(\rho \mathbf{B} \times \frac{d\mathbf{U}_{sw}}{dt} + \mathbf{B} \times \nabla p \right) \tag{56}$$

Furthermore, since the solar wind plasma is perfectly conductive, we have $\mathbf{E}_{sw} + \mathbf{U}_{sw} \times \mathbf{B} = 0$. Using the identity $(\mathbf{a} \times \mathbf{b}) \cdot (\mathbf{c} \times \mathbf{d}) = (\mathbf{a} \cdot \mathbf{c})(\mathbf{b} \cdot \mathbf{d}) - (\mathbf{a} \cdot \mathbf{d})(\mathbf{b} \cdot \mathbf{c})$ (known as Binet-Cauchy's identity), we can more easily express $\mathcal{P}$ and obtain

$$\mathcal{P} \sim -\rho \mathbf{U}_{sw} \cdot \frac{d\mathbf{U}_{sw}}{dt} \tag{57}$$

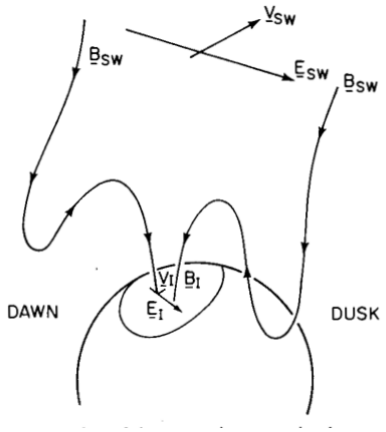

FIGURE 12 – Illustration of the solar wind-ionosphere magnetic connection (region I), for an interplanetary magnetic field pointing south.

in the extremely simplified case where we have neglected the effect of the pressure gradient and considered that $\mathbf{B}$ and $\mathbf{U}_{sw}$ were perpendicular or almost perpendicular. We can see that it is the variation in kinetic energy of the solar wind that is the source of the system's electrical energy : it functions like an MHD generator connected to the ionospheric system, which acts as a passive load.

The electrical power supplied by the solar wind is transmitted along field lines to the ionosphere, where it circulates and forms a system of currents $\mathbf{J} = \sigma \mathbf{E}_{iono}$, consisting of two components : a Pedersen component aligned with the ionospheric electric field $\mathbf{E}_{iono}$ (meridional currents), and a Hall component circulating perpendicular to $\mathbf{E}_{iono}$ and $\mathbf{B}$ (zonal currents). We can see (see fig.12) that the field $\mathbf{E}_{iono}$ is directed, like $\mathbf{E}_{sw}$, from morning to evening. We can also see that it will be more intense than the interplanetary field, since the magnetic field lines (isopotentials) converge as they approach the Earth. The factor between $\mathbf{E}_{iono}$ and $\mathbf{E}_{sw}$ depends on the precise geometry of the field lines (factor ~ 50).

Figure 13 shows the geometry of the coupling between the ionosphere and the inner magnetosphere. This coupling works in a similar way to that described above for the solar wind, except that it is the convective motions of the magnetospheric plasma that generate the current. As before, the ionosphere essentially acts as a passive load receiving this current.

Since magnetospheric convection movements are directed from the tail of the magnetosphere towards the Sun, i.e. in the opposite direction to the convection movement of the solar wind, the electric field projected onto the ionosphere will be oriented from evening to morning (see figure), and the resulting ionospheric current will flow in the opposite direction to that of the polar horn directly connected to the solar wind. The current

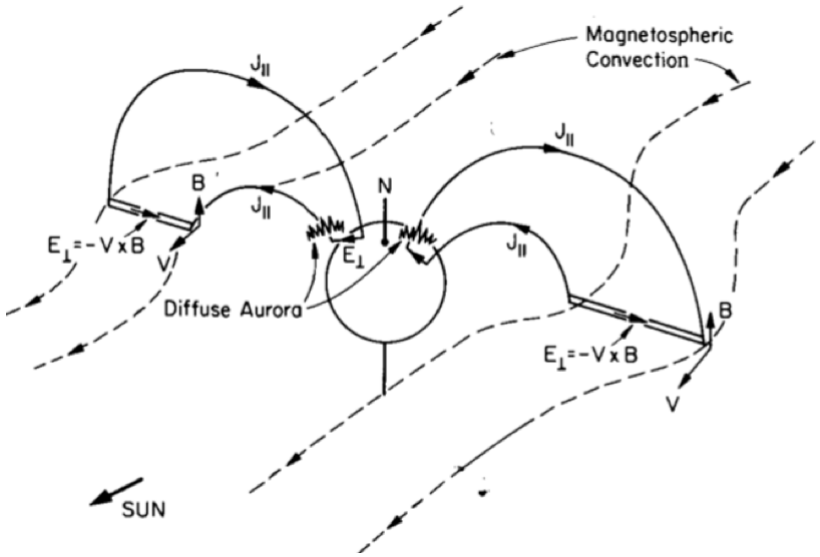

FIGURE 13 – Schematic representation of the magnetic and electrical coupling between the magnetosphere and ionosphere (region II)

system produced will again be separated into Pedersen and Hall components (flowing in the meridional and zonal directions respectively), but the direction of flow is reversed compared to the currents in region I.

The currents aligned with the magnetic field, upon entering the atmosphere, will cause the excitation of atoms or molecules (electron-neutral collisions, which we have seen are responsible for ionospheric conductivity effects), which, upon de-excitation, emit radiation responsible for the phenomenon of diffuse and continuous aurora borealis. These currents are called Birkeland currents, in honour of the Norwegian physicist Kristian Birkeland, who, observing the disturbance of compasses during intense aurora borealis, had hypothesised their existence. During periods of solar calm, Birkeland currents carry approximately 10^5 A. During solar magnetic storms, their intensity can reach several million amperes.

Fig. 14 presents an overview of the ionospheric current system at high latitudes. It shows Birkeland currents (aligned with **B** and connecting to high altitudes), Pedersen and Hall currents, and the reversal of their direction when passing from region I (polar horn connected to the solar wind) to region II (connected to the inner magnetosphere).

3 Bibliography

— *Introduction to Ionospheric Physics*, Heny Rishbeth, Owen K. Garriott, Academic Press, 1969

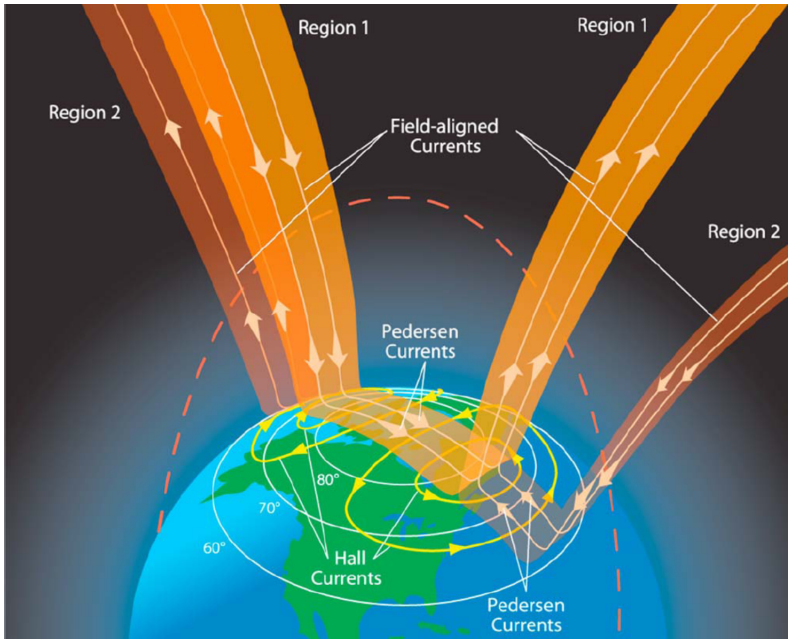

FIGURE 14 – Overview of the ionospheric current system at high latitudes.

— *The Earth's Ionosphere, Plasma Physics and Electrodynamics.* Michael C. Kelley, International Geophysics Series, Vol. 43, 1996

— *The ionospheric E-layer and F-layer dynamos - a tutorial review.* Henry Rishbeth, Journal of Atmospheric and Solar-Terrestrial Physics, Vol. 59, 1997